

Perspective on probing metallic ferromagnetism with electrons (invited)

D. T. Pierce^{a)}*Center for Nanoscale Science and Technology, NIST, Gaithersburg, Maryland 20899, USA*

(Presented 17 November 2010; received 24 September 2010; accepted 5 November 2010; published online 21 March 2011)

This article presents a brief review of insights gained about metallic ferromagnetism using spin-polarized electrons as probes. In ferromagnets, the electronic structure is spin-polarized because of the exchange interaction, allowing the fundamental properties of ferromagnets to be measured by spin-polarized versions of techniques such as photoemission and inverse photoemission. Not only can the static electronic structure be measured, but also magnetic excitations can be measured using spin polarized versions of techniques like electron energy loss spectroscopy. Further, since the polarization is a vector, mapping it maps the underlying domain structure of the ferromagnet. A brief discussion is presented of both early and contemporary applications of spin polarized measurement techniques and what has been learned. [doi:10.1063/1.3537960]

I. INTRODUCTION

Various types of electron spectroscopy and microscopy have provided us with enormous insight into metallic ferromagnetism. Since the ordering of electron spins is at the heart of ferromagnetism, it is not surprising that electron probes that give information about the spin state are particularly useful. In this brief review, I limit the scope of the discussion to electron probes where either the incident electron is spin polarized or the spin polarization of electrons emitted after excitation is measured. I do not discuss other very useful probes of ferromagnetism, also involving electrons, such as x-ray magnetic circular dichroism and photoemission electron microscopy in which the spin dependence relies on the incident photon polarization. An in depth discussion of such photon based techniques and further exposition of spin-polarized electron probes can be found elsewhere.¹

The elemental room temperature ferromagnetic metals Fe, Co, Ni, and their alloys dominate technological applications, particularly in electronics and information storage. The discovery of giant magnetoresistance^{2,3} (GMR) has led to an explosion of applications using GMR and subsequently tunneling magnetoresistance, most dramatically in hard drive read heads. Ferromagnetic metals are also important in conjunction with semiconductor spintronics for spin injection through a tunnel barrier or over a Schottky barrier, and many device concepts rely on spin filtering by a ferromagnetic layer or spin valve. The use of currents to reorient magnetization by spin transfer torque opens up the possibility of new devices for memory, and other spintronics applications.

II. SPIN DEPENDENT ELECTRONIC STRUCTURE

Spin dependent photoemission spectroscopy (PES) and inverse photoemission spectroscopy (IPES) have become important probes of the electronic structure of ferromagnets. In PES an incident photon excites an electron which is detected.

Measuring the spin requires a spin analyzer. Spin analyzers used to measure the spin polarization of photoemitted electrons rely on an asymmetry in the scattering of electrons from a target caused by either the spin-orbit interaction or the exchange interaction. Traditionally, spin analysis has been achieved with a Mott detector^{4,5} in which an asymmetry due to the spin-orbit interaction is measured when electrons are scattered at high energy (≈ 100 keV) from a high atomic number target such as gold. Numerous configurations of the Mott detector have been developed, including those that operate at lower energy.⁶⁻⁹ Spin analyzers based on exchange scattering at a ferromagnetic surface can be relatively efficient and are particularly well suited to experiments where the electron beam is well resolved in energy and angle.¹⁰⁻¹²

Early spin polarized photoemission experiments used 100 keV Mott scattering to measure the polarization of the total electron current near photothreshold without energy analysis.¹³⁻¹⁵ The polarization is defined as $P = (n^+ - n^-)/(n^+ + n^-)$, where $n^+(n^-)$ are the number of electrons with spin parallel (antiparallel) to a quantization direction. Here we define n^+ as the number of electrons with spin in the direction of the majority electrons in the ferromagnet. The polarization of photoelectrons emitted from a Ni(100) single crystal near photothreshold was found to be negative.¹⁴ This means that the electrons at the Fermi energy, those excited to photothreshold, are predominantly minority spin as expected from band structure calculations for Ni. Spin polarized photoemission measurements soon developed to resolve energy, angle, and spin.¹⁶ Such detailed measurements of the spin dependent electronic structure of Ni(110) highlight the importance of correlation effects which are not adequately treated in band calculations.¹⁷ The reduction in d bandwidth is found to be larger in the majority spin spectra, and the exchange splitting is found to be k -dependent. Of particular interest is the behavior at finite temperatures. In Ni, the exchange splitting near T_C was observed to collapse,¹⁶ but in Fe the d band peak positions remained nearly stationary with increasing temperature while the spin polarization of the peaks decreased.¹⁸ Spin-resolved two-photon photoemission using image potential states as sensors

^{a)}Author to whom correspondence should be addressed. Electronic mail: pierce@nist.gov.

recently probed the magnetic order in a two monolayer Fe film below and above the Curie temperature.¹⁹ Although the long range magnetic order vanishes at the Curie temperature, the data give clear evidence for local magnetic order persisting well above T_C . Such results challenge electronic structure calculations which must go beyond an independent particle approximation to obtain a unified picture of an itinerant ferromagnet with strong electron correlation.

Early spin polarized photoemission measurements, which established the predominance of minority electrons at the Fermi level, seemed to conflict with spin dependent tunneling results²⁰ from Ni into a superconducting Al thin film, which showed that the current carriers were predominantly majority spin electrons. While puzzling at the time, we now understand that the polarization of the tunneling current includes factors of the Fermi velocity and is different than the polarization of the density of states probed in photoemission.²¹ This understanding of the variety of polarizations is important in present day investigations of spintronic devices.

Inverse photoemission spectroscopy can measure the spin-dependent electronic structure of the unfilled states if the electron beam exciting the photon is spin-polarized. While there are a number of ways to form a spin-polarized electron beam,²² the best source of spin-polarized electrons relies on photoemission from negative electron affinity GaAs. In the GaAs polarized electron source, circularly polarized light excites electrons from the top of the spin-orbit split valence band to the bottom of the conduction band. Selection rules are such that up to 50% polarization is possible.²³ Polarization approaching 100% is possible if the degeneracy of the light-hole and heavy-hole bands at the valence band maximum is lifted, for example, by straining the GaAs layer.²⁴ The ability to modulate the spin-polarization of the electron beam parallel or antiparallel to the sample magnetization, by simply switching the helicity of the incident photons, makes it possible to pick out small spin-dependent effects. The same type of optical pumping in GaAs is important for creating and studying

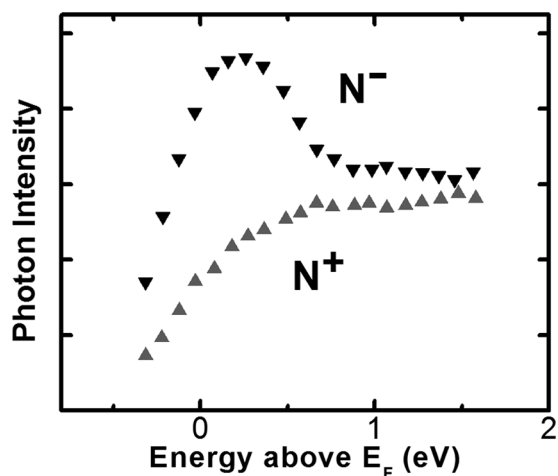


FIG. 1. Inverse photoemission spectra for Ni(110) at an angle of incidence of 20° show the photon intensity resulting from 9.7 eV transitions of incident spin-polarized electrons to unfilled states just above the Fermi level. Reprinted with permission from J. Unguris, A. Seiler, R. J. Celotta, D. T. Pierce, P. D. Johnson, and N. V. Smith, Phys. Rev. Lett. 49, 1047 (1982). Copyright © 1982, The American Physical Society.

spin-polarized electrons in materials and devices for spintronics.²⁵

The first spin-polarized IPES of a Ni(110) surface, shown in Fig. 1,²⁶ exhibits a peak in the photon intensity N^- , which is due to transitions of incident minority spin electrons to final states above E_F , but not in the N^+ photon intensity. This difference clearly indicates that the unfilled d -band states in Ni that give rise to the ferromagnetism are of minority character. In subsequent measurements, the unfilled magnetic states in Ni along the $X-W$ direction were measured as a function of temperature with spin-polarized IPES.²⁷ The data show the minority and majority spin peaks merging with increasing temperature with the exchange splitting decreasing as the bulk magnetization.²⁸ Spin-polarized inverse photoemission studies were also able to determine the spin-dependent features of surface states and resonances, such as crystal-induced surface states and image-potential-induced surface states.²⁹ The spin dependent properties at the surface vacuum interface, and likewise at an interface with another material, can be quite different from the bulk and must be considered when seeking to understand, for example, spin transport across an interface.

III. SPIN-DEPENDENT MEAN FREE PATHS

Spin-polarized electron measurements show that the electron mean free path is spin dependent, which causes ferromagnetic metals to act as spin filters. Indications that the inelastic electron mean free path is spin dependent were first observed in measurements of the spin polarization of photoemission³⁰ and secondary electron emission.^{31,32} A significant enhancement of the spin polarization was found for secondary electron kinetic energies less than about 5 eV seen in measurements of Ni(110) (Ref. 32) shown in Fig. 2. Without spin filtering, one would expect the secondary electron polarization to reflect the polarization of the valence band of Ni given by $P = n_B/n$ where $n_B = 0.51$ is the spin part of the magnetic moment per atom in Bohr magnetons at room temperature T , $T/T_C = 0.48$, and $n = 10$ is the number of valence electrons per Ni atom. In

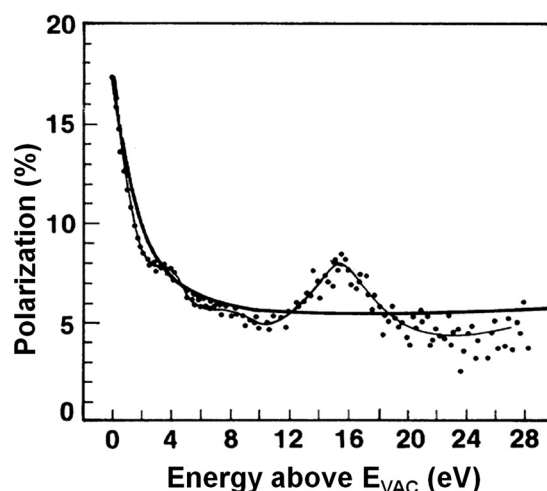


FIG. 2. Spin polarization of secondary electrons from Ni(110) as a function of kinetic energy. The heavy solid line is the calculated spin polarization including scattering of minority-spin electrons into empty d states. Reprinted with permission from D. R. Penn, S. P. Apell, and S. M. Girvin, Phys. Rev. Lett. 55, 518 (1985). Copyright © 1985, The American Physical Society.

Fig. 2, above 5 eV, a polarization of about 5% at higher kinetic energy is observed as expected, except for some band structure effects³³ around 15 eV. The key to understanding the increase in the polarization below 5 eV by about a factor of 3 is that minority spins are preferentially scattered out of the secondary electron distribution due to the excess of unfilled minority spin states.³⁴ The positive polarization from the majority electrons is thus enhanced.

The electron mean free path is also quite short in the energy range of experiments discussed here. Thus, the probing depth of electron spectroscopies, which is determined by the inelastic mean free path of incident or emitted electrons, is typically only a few atomic layers. Because of this, the spectroscopic data can contain information from both bulk-derived and surface-derived states and some care is necessary to distinguish them.

The preferential filtering of minority spin electrons was clearly demonstrated in spin-polarized photoemission measurements of thin Fe films on Cu.³⁵ Because the peaks in the spectra due to photoelectrons from the Cu substrate and the Fe overlayer occur at different energies, it was possible to determine that the electrons originating in the Cu were spin polarized after they had traversed the Fe overlayer. If the inelastic mean free path (which is the attenuation length if elastic scattering is negligible) is different for majority and minority spin electrons, the individual spin currents measured in photoemission can be written $I^{+-} = (1/2)I_0 \exp(-d/\lambda^{+-})$, where I^+ (I^-) are the measured electron intensities with spin parallel (antiparallel) to the majority spins in the ferromagnet, d is the distance, and I_0 is the unpolarized intensity from the Cu. The selective absorption of minority spin electrons in the Fe overlayer leads to a positive polarization of the Cu peak. The ratio of the majority electron mean free path $\lambda^+ = 0.58$ nm to the minority electron mean free path $\lambda^- = 0.46$ nm was found to be $\lambda^+/\lambda^- = 1.25$ for an electron energy of 12 eV above the Fermi energy.

Spin filtering is important in solid state spintronic devices designed to manipulate spin-polarized currents. In the spin valve transistor³⁶ ballistic electrons were injected from the Si emitter over a Schottky barrier into the spin valve base and collected over another Schottky barrier in the Si collector. The electron energy of interest for spin filtering by the spin valve base in this device is about 1 eV above E_F . Measurements can be made of the mean free path for electrons with energy 1 to 2 eV above E_F if the injection into the ferromagnetic base is from the emitter through a tunnel barrier and the bias between the emitter and the base is varied. For example, at an energy of 1.4 eV above E_F , $\lambda^+ = 5.0$ nm and $\lambda^- = 0.9$ nm for $\text{Co}_{84}\text{Fe}_{16}$, making it a better spin filter than $\text{Ni}_{81}\text{Fe}_{19}$.³⁷ A recent application of spin filtering demonstrated coherent spin transport in Si where spin-dependent hot electron filtering through ferromagnetic films was used for both spin injection and spin detection.³⁸

IV. SPIN WAVES

Spin-polarized electron scattering from surfaces is proportional to the ferromagnetic order at the surface and therefore can be used to measure surface hysteresis curves,^{39,40} the temperature dependence of the magnetization, and the

excitation of spin waves. When an electron scatters from a surface, the unpolarized Coulomb scattering dominates. Because the incident electron polarization can be repeatedly reversed without otherwise disturbing the beam by simply reversing the helicity of the light exciting the electrons in the GaAs photocathode, it is possible using lock-in techniques to measure a very small spin dependent asymmetry on a large background of Coulomb scattering.

The decrease in the magnetization of a ferromagnet with temperature up to about $0.3T_C$, is due to the excitation of long wavelength spin waves or magnons. The temperature dependence follows the Bloch $T^{3/2}$ law $M(T)/M(0) = 1 - \kappa BT^{3/2}$, where B is a constant, and $\kappa = 1$ for the bulk. At the surface, the temperature dependence can be different. Because a spin wave becomes a standing wave with an antinode at the surface, the spin deviation is twice as large as the bulk. The decrease in the surface magnetization with temperature was predicted to decrease with the same power law but with $\kappa = 2$ and hence faster than the bulk.^{41,42} Several years after the predictions were made, they were tested⁴³ by measuring the spin-dependent scattering asymmetry of a polarized electron beam. The scattering asymmetry, proportional to $M(T)$, followed a $T^{3/2}$ fit to the data with $\kappa = 3$. The larger than predicted κ could be explained if the exchange coupling perpendicular to the surface layer is less than the intraplanar exchange.⁴⁴ Subsequent measurements showed that adsorbates on the surface can alter the exchange interaction parallel and perpendicular to the surface and cause κ to be greater than or less than 2.⁴⁵

Measuring the spin wave dispersion of shorter wavelength spin waves in ferromagnetic surfaces and thin films is a significant challenge but is possible with polarized electrons. For some years spin polarized electron energy loss spectroscopy (SPEELS) has been used to measure Stoner excitations, an excitation of an electron from a filled state in a majority band to an empty state in the minority spin band.^{46,47} Recently, in a SPEELS experiment with very high energy resolution and low kinetic energy of the incident electrons, the spin wave dispersion was measured without spin analysis of the scattered electrons.⁴⁸ It is possible to distinguish spin excitations from vibrational excitations by varying the polarization of the incident beam. Only incident electrons with spin parallel to the minority spins in the sample I^- can excite spin waves. This process is illustrated in Fig. 3(a) for electrons scattering from an 8 monolayer (ML) hcp Co film.⁴⁹ The spin wave dispersion from many such measurements is shown in Fig. 3(b) all the way to the boundary of the surface Brillouin zone. The figure also includes previous measurements from an 8 ML fcc Co film.⁴⁸ The dashed lines, which are the dispersion relations for an acoustic surface spin wave mode calculated in the nearest-neighbor Heisenberg approximation, are in good agreement with the data. The full width at half maximum of the hcp Co spin wave peak, corrected for experimental broadening, increases with scattering wave vector indicating a short lifetime explained by rapid decay into single particle Stoner excitations.⁵⁰

V. SURFACE AND INTERFACE ANISOTROPY

In this and the next two sections, we discuss two very powerful techniques to image magnetization, and demonstrate

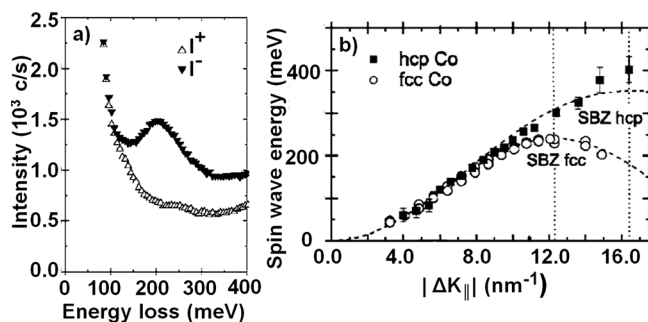


FIG. 3. (a) SPEELS spectra for I^+ and I^- measured for a wave vector transfer of 8.8 nm^{-1} on an 8 ML Co film. (b) Spin wave dispersion for 8 ML hcp Co on W(110) and 8 ML fcc Co on Cu(100) measured by SPEELS. The dashed lines are the dispersion relations for an acoustic surface spin wave mode calculated using a nearest-neighbor Heisenberg model. Reprinted with permission from M. Etzkom, P. S. Anil Kumar, W. Tang, Y. Zhang, and J. Kirschner, Phys. Rev. B 72, 184420 (2005). Copyright © 2005, The American Physical Society.

their efficacy with some examples. The first is spin-polarized low energy electron microscopy (SPLEEM),⁵¹ which utilizes a spin-polarized electron beam from a GaAs photocathode directed to the sample surface at normal incidence. The diffracted specular beam is magnified in an optical column to form a real space image of the sample surface. Under appropriate diffraction conditions, single layer height differences are readily resolved. Contributions to the magnetic contrast come from the spin dependent inelastic mean free path discussed in Sec. III and the quasielastic exchange scattering discussed in Sec. IV. Again, modulation of the spin polarization of the incident electrons allows the isolation of spin dependent effects. SPLEEM can provide a magnetic image while following the thin film growth layer by layer.

The strengths of SPLEEM are illustrated by measurements of a spin reorientation transition, which occurs due to changes in the balance of contributions to the total magnetic anisotropy. The reduced coordination at the surface of a ferromagnet can cause the surface anisotropy to be different from the bulk. The anisotropy at a surface or interface is a delicate balance of electronic and structural effects such as strain. A large uniaxial anisotropy, predicted for some ferromagnetic films, causes the easy axis to be perpendicular to the surface.⁵² As the film thickness is increased, the shape anisotropy becomes stronger and causes a spin reorientation transition forcing the magnetization to lie in the plane of the film. The anisotropy at interfaces of thin films forming multilayers can be exploited to make materials with perpendicular anisotropy such as CoPt and CoPd.⁵³

SPLEEM provides a very sensitive way to observe a spin reorientation transition. As an example, Co on Ru(0001) grows layer-by-layer without intermixing. SPLEEM measurements reveal two spin reorientation transitions.⁵⁴ The first monolayer is magnetized in plane; with the second layer added, the magnetization orients perpendicular to the plane of the film; and with the third and more layers the magnetization is again in plane. Only for the 2 ML film does the interplay between strain, interface, and surface effects lead to a perpendicular magnetization.

VI. MAGNETIC NANOSTRUCTURE

Another magnetic imaging technique is scanning electron microscopy with polarization analysis (SEMPA),⁵⁵ in

which the spin polarization of secondary electrons excited with a finely focused scanning electron microscope (SEM) beam is measured to give high resolution images of the magnetic microstructure. SEMPA measures the direction of the magnetization directly, independently of, but along with the usual SEM topography image. The spatial resolution of SEMPA is 10 nm, and the probing depth is 1 nm.

SEMPA can readily image the magnetic nanostructure of a wide variety of materials and devices. When the energy to form a domain wall is less than the stray field energy, the ferromagnet breaks up into domains. In sub 100 nm structures of soft ferromagnetic materials, the energy cost to support multidomain structures becomes prohibitive. Circular nanodisks, depending on the ratio of thickness to diameter, can be single domain with magnetization in plane, out of plane, or in a vortex configuration. SEMPA was recently used to map out a phase diagram for such structures.⁵⁶ The vortex configuration is described by its chirality, the sense of the circulation of the magnetization, and its polarity, the direction of the perpendicular magnetization in the vortex core. SEMPA measurements of the in-plane and out-of-plane components of the magnetization were able to determine the vortex chirality and polarity in a single measurement.⁵⁷

VII. COUPLING OF MAGNETIC LAYERS

SEMPA measurements of indirect exchange in magnetic multilayers quantify the dramatic oscillatory behavior. Ferromagnetic layers separated by a nonmagnetic layer can be coupled ferromagnetically or antiferromagnetically, that is, with magnetizations respectively parallel or antiparallel. In high quality multilayers, the coupling oscillates with increasing thickness of the spacer layer.⁵⁸ Giant magnetoresistance was discovered in such antiferromagnetically coupled films.^{2,3} When a magnetic field causes parallel alignment, there is a large drop in resistance. SEMPA measurements on samples with nearly perfect interfaces confirmed theoretical models for the strength and periodicity of the oscillatory coupling. Theory suggests that the periods are determined by the extremal spanning vectors of the spacer layer Fermi surface.⁵⁹ The strength depends on the Fermi surface geometry and the reflection amplitudes for electrons scattering at the interfaces between the spacer layer and the ferromagnetic layers that produce quantum well states.⁶⁰

An example of the precise determination of the periods of oscillatory coupling is seen in measurements of a trilayer consisting of an Fe(100) whisker, a linearly increasing thickness (wedge) Au spacer layer, and an Fe top layer.⁶¹ The Fe(100)/Au wedge/Fe overlayer structure is shown in Fig. 4. A key to these measurements is the very flat Fe whisker with terraces of order $1 \mu\text{m}$.⁶² The Au growth is layer-by-layer. In the SEMPA images of Fig. 4, white (black) indicates that M_x is directed to the $+x(-x)$ direction while the gray indicates that $M_x = 0$; a similar definition applies to M_y . The periods of the coupling were determined to be 2.48 ± 0.05 layers and 8.6 ± 0.3 layers in good agreement with expectations from the Au Fermi surface.⁵⁹ Similar very precise measurements were made of the periods of oscillation for the case of a Cr spacer layer.^{63,64} The strength of the coupling of Fe/Au/Fe

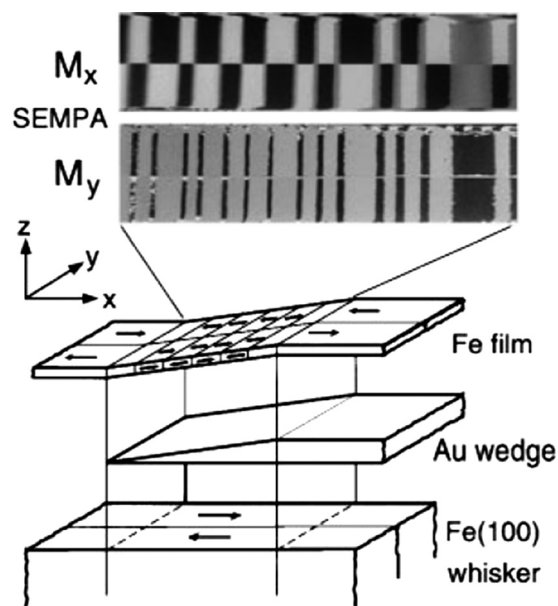


FIG. 4. Schematic diagram of the sample configuration consisting of the Fe(001) whisker, a wedge-shaped Au spacer layer, and a thin Fe top layer. The SEMPA images of the M_x and M_y components of the magnetization display the oscillatory coupling with two periods. Reprinted with permission from J. Unguris, R. J. Celotta, D. A. Tulchinsky, and D. T. Pierce, *J. Magn. Mater.* **198–199**, 396 (1999). Copyright © 1999, Elsevier B.V.

was determined with a combination of magneto-optic Kerr measurements in a magnetic field and SEMPA and reflection high-energy electron diffraction measurements to monitor the quality of the trilayer structure.⁶⁵ The coupling strengths measured for these nearly perfect samples substantially agreed with calculations.^{66,67}

VIII. OUTLOOK

Spin polarized electron spectroscopies have contributed greatly to our understanding of metallic ferromagnetism and should continue to do so. Further investigations of ultrafast magnetization dynamics are expected.⁶⁸ Spin polarized photoemission is being applied to numerous nonmagnetic materials. Spin-resolved two photon photoemission has measured spin injection efficiency and spin transport properties in an organic semiconductor.⁶⁹ Spin polarized photoemission has shown a spin-orbit split and spin-polarized Fermi surface in quasi-free-standing graphene.⁷⁰ Finally, topological insulators are now being investigated by spin-resolved photoemission.^{71,72}

ACKNOWLEDGMENTS

Helpful discussions with J. Unguris and M. D. Stiles are gratefully acknowledged.

¹J. Stöhr and H. C. Siegmann, *Magnetism: From Fundamentals to Nano-scale Dynamics* (Springer-Verlag, Berlin, 2006).

²M. N. Baibich, J. M. Broto, A. Fert, F. Nguyen Van Dau, F. Petroff, P. Eitenne, G. Creuzet, A. Friederich, and J. Chazelas, *Phys. Rev. Lett.* **61**, 2472 (1988).

³J. Barnás, A. Fuss, R. E. Camley, P. Grünberg, and W. Zinn, *Phys. Rev. B* **42**, 8110 (1990).

⁴N. F. Mott, *Proc. R. Soc. London A* **124**, 425 (1929).

⁵J. Kessler, *Polarized Electrons*, 2nd ed. (Springer, Berlin, 1985).

⁶D. T. Pierce, R. J. Celotta, M. H. Kelley, and J. Unguris, *Nucl. Instrum. Methods Phys. Res. A* **266**, 550 (1988).

⁷L. G. Gray, M. W. Hart, F. B. Dunning, and G. K. Walters, *Rev. Sci. Instrum.* **55**, 88 (1984).

⁸J. Kirschner and R. Feder, *Phys. Rev. Lett.* **42**, 1008 (1979).

⁹M. R. Scheinfein, D. T. Pierce, J. Unguris, J. J. McClelland, R. J. Celotta, and M. H. Kelley, *Rev. Sci. Instrum.* **60**, 1 (1989).

¹⁰D. Tillmann, R. Thiel, and E. Kisker, *Z. Phys. B* **77**, 1 (1989).

¹¹A. Winkelmann, D. Hartung, H. Engelhard, C.-T. Chiang, and J. Kirschner, *Rev. Sci. Instrum.* **79**, 083303 (2008).

¹²C. Jozwiak, J. Graf, G. Lebedev, N. Andresen, A. K. Schmid, A. V. Fedorov, F. El Gabaly, W. Wan, A. Lanzara, and Z. Hussain, *Rev. Sci. Instrum.* **81**, 053904 (2010).

¹³U. Bänninger, G. Busch, M. Campagna, and H. C. Siegmann, *Phys. Rev. Lett.* **25**, 585 (1970).

¹⁴W. Eib and S. F. Alvarado, *Phys. Rev. Lett.* **37**, 444 (1976).

¹⁵M. Campagna, D. T. Pierce, F. Meier, K. Sattler, and H. C. Siegmann, *Adv. Electron. Electron Phys.* **41**, 113 (1976).

¹⁶H. Hopster, R. Raue, G. Güntherodt, E. Kisker, R. Clauberg, and M. Campagna, *Phys. Rev. Lett.* **51**, 829 (1983).

¹⁷K. Ono, A. Kakizaki, K. Tanaka, K. Shimada, Y. Saitoh, and T. Sendohda, *Solid State Commun.* **107**, 153 (1998).

¹⁸E. Kisker, K. Schröder, W. Gudat, and M. Campagna, *Phys. Rev. B* **31**, 329 (1985).

¹⁹M. Pickel, A. B. Schmidt, M. Weinelt, and M. Donath, *Phys. Rev. Lett.* **104**, 237204 (2010).

²⁰P. M. Tedrow and R. Meservey, *Phys. Rev. Lett.* **26**, 192 (1971).

²¹I. I. Mazin, *Phys. Rev. Lett.* **83**, 1427 (1999).

²²D. T. Pierce, in *Experimental Methods in the Physical Sciences*, edited by F. B. Dunning and R. G. Hulet (Academic, San Diego, 1995), Vol. 29A.

²³D. T. Pierce, R. J. Celotta, G. C. Wang, W. N. Unertl, A. Galejs, C. E. Kuyatt, and S. R. Mielczarek, *Rev. Sci. Instrum.* **51**, 478 (1980).

²⁴T. Maruyama, E. L. Garwin, R. Prepost, and G. H. Zapalac, *Phys. Rev. B* **46**, 4261 (1992).

²⁵J. M. Kikkawa and D. D. Awschalom, *Phys. Rev. Lett.* **80**, 4313 (1998); I. Malajovich, J. M. Kikkawa, D. D. Awschalom, J. J. Berry, and N. Samarth, *ibid.* **84**, 1015 (2000).

²⁶J. Unguris, A. Seiler, R. J. Celotta, D. T. Pierce, P. D. Johnson, and N. V. Smith, *Phys. Rev. Lett.* **49**, 1047 (1982).

²⁷M. Donath and V. Dose, *Europhys. Lett.* **9**, 821 (1989).

²⁸W. von der Linden, M. Donath, and V. Dose, *Phys. Rev. Lett.* **71**, 899 (1993).

²⁹M. Donath, *Surf. Sci. Rep.* **520**, 253 (1994).

³⁰A. Bringer, M. Campagna, R. Feder, W. Gudat, E. Kisker, and E. Kuhlmann, *Phys. Rev. Lett.* **42**, 1705 (1979).

³¹J. Unguris, D. T. Pierce, A. Galejs, and R. J. Celotta, *Phys. Rev. Lett.* **49**, 72 (1982).

³²H. Hopster, R. Raue, E. Kisker, G. Güntherodt, and M. Campagna, *Phys. Rev. Lett.* **50**, 70 (1983).

³³E. Tamura and R. Feder, *Phys. Rev. Lett.* **57**, 759 (1986).

³⁴D. R. Penn, S. P. Apell, and S. M. Girvin, *Phys. Rev. Lett.* **55**, 518 (1985).

³⁵D. P. Pappas, K. P. Kämper, B. P. Miller, H. Hopster, D. E. Fowler, C. R. Brundle, A. C. Luntz, and Z. X. Shen, *Phys. Rev. Lett.* **66**, 504 (1991).

³⁶D. J. Monsma, R. Vluters, and J. C. Lodder, *Science* **281**, 407 (1998).

³⁷S. van Dijken, X. Jiang, and S. S. P. Parkin, *Phys. Rev. B* **66**, 094417 (2002).

³⁸I. Appelbaum, B. Huang, and D. J. Monsma, *Nature* **447**, 295 (2007).

³⁹R. J. Celotta, D. T. Pierce, G.-C. Wang, S. D. Bader, and G. P. Felcher, *Phys. Rev. Lett.* **43**, 728 (1979).

⁴⁰D. T. Pierce, and R. J. Celotta, *Adv. Electron. Electron Phys.* **56**, 219 (1981).

⁴¹G. T. Rado, *Bull. Am. Phys. Soc.* **112**, 127 (1957).

⁴²D. L. Mills and A. A. Maradudin, *J. Phys. Chem. Solids* **28**, 1855 (1967).

⁴³D. T. Pierce, R. J. Celotta, J. Unguris, and H. C. Siegmann, *Phys. Rev. B* **26**, 2566 (1982).

⁴⁴J. Mathon and S. B. Ahmad, *Phys. Rev. B* **37**, 660 (1988).

⁴⁵D. Mauri, D. Scholl, H. C. Siegmann, and E. Kay, *Phys. Rev. Lett.* **61**, 758 (1988).

⁴⁶J. Kirschner, D. Rebenstorff, and H. Ibach, *Phys. Rev. Lett.* **53**, 698 (1984).

⁴⁷D. L. Abraham and H. Hopster, *Phys. Rev. Lett.* **62**, 1157 (1989).

⁴⁸R. Vollmer, M. Etzkorn, P. S. Anil Kumar, H. Ibach, and J. Kirschner, *Phys. Rev. Lett.* **91**, 147201 (2003).

- ⁴⁹M. Etzkorn, P. S. Anil Kumar, W. Tang, Y. Zhang, and J. Kirschner, *Phys. Rev. B* **72**, 184420 (2005).
- ⁵⁰A. T. Costa, Jr., R. B. Muniz, and D. L. Mills, *Phys. Rev. B* **69**, 064413 (2004).
- ⁵¹N. Rougemaille and A. K. Schmid, *Eur. Phys. J. Appl. Phys.* **50**, 20101 (2010).
- ⁵²J. G. Gay and R. Richter, *Phys. Rev. Lett.* **56**, 2728 (1986).
- ⁵³P. F. Carcia, A. D. Meinhardt, and A. Suna, *Appl. Phys. Lett.* **47**, 178 (1985).
- ⁵⁴F. El Gabaly, S. Gallego, C. Muñoz, L. Szunyogh, P. Weinberger, C. Klein, A. K. Schmid, K. F. McCarty, and J. de la Figuera, *Phys. Rev. Lett.* **96**, 147202 (2006).
- ⁵⁵M. R. Scheinfein, J. Unguris, M. H. Kelley, D. T. Pierce, and R. J. Celotta, *Rev. Sci. Instrum.* **61**, 2501 (1990).
- ⁵⁶S.-H. Chung, R. D. McMichael, D. T. Pierce, and J. Unguris, *Phys. Rev. B* **81**, 024410 (2010).
- ⁵⁷S.-H. Chung, D. T. Pierce, and J. Unguris, *Ultramicroscopy* **110**, 177 (2010).
- ⁵⁸S. S. P. Parkin, N. More, and K. P. Roche, *Phys. Rev. Lett.* **64**, 2304 (1990).
- ⁵⁹P. Bruno and C. Chappert, *Phys. Rev. Lett.* **67**, 1602 (1991).
- ⁶⁰M. D. Stiles, *Phys. Rev. B* **48**, 7238 (1993).
- ⁶¹J. Unguris, R. J. Celotta, D. A. Tulchinsky, and D. T. Pierce, *J. Magn. Mater.* **198–199**, 396 (1999).
- ⁶²J. A. Stroschio and D. T. Pierce, *J. Vac. Sci. Technol. B* **12**, 1783 (1994).
- ⁶³J. Unguris, R. J. Celotta, and D. T. Pierce, *Phys. Rev. Lett.* **67**, 140 (1991).
- ⁶⁴D. T. Pierce, J. Unguris, R. J. Celotta, and M. D. Stiles, *J. Magn. Mater.* **200**, 290 (1999).
- ⁶⁵J. Unguris, R. J. Celotta, and D. T. Pierce, *Phys. Rev. Lett.* **79**, 2734 (1997).
- ⁶⁶M. D. Stiles, *J. Appl. Phys.* **79**, 5805 (1996).
- ⁶⁷J. Opitz, P. Zahn, J. Binder, and I. Mertig, *Phys. Rev. B* **63**, 094418 (2001).
- ⁶⁸M. Cinchetti, M. Sánchez Albaneda, D. Hoffmann, T. Roth, J.-P. Wüsterberg, M. Krauss, O. Andreyev, H. C. Schneider, M. Bauer, and M. Aeschlimann, *Phys. Rev. Lett.* **97**, 1777201 (2006); B. Koopmans, G. Malinowski, F. Dalla Longa, D. Steiauf, M. Fähnle, T. Roth, M. Cinchetti, and M. Aeschlimann, *Nat. Mater.* **9**, 259 (2010).
- ⁶⁹M. Cinchetti, K. Heimer, J.-P. Wüstenberg, O. Andreyev, M. Bauer, S. Lach, C. Ziegler, Y. Gao, and M. Aeschlimann, *Nat. Mater.* **8**, 115 (2009).
- ⁷⁰A. Varykhalov, J. Sánchez-Barriga, A. M. Shikin, C. Biswas, E. Vescovo, A. Rybkin, D. Marchenko, and O. Rader, *Phys. Rev. Lett.* **101**, 157601 (2008).
- ⁷¹D. Hsieh, Y. Xia, L. Wray, D. Qian, A. Pal, J. H. Dil, J. Osterwalder, F. Meier, G. Bihlmayer, C. L. Kane, Y. S. Hor, R. J. Cava, and M. Z. Hasan, *Science* **323**, 919 (2009).
- ⁷²D. Hsieh, Y. Xia, D. Qian, L. Wray, J. H. Dil, F. Meier, J. Osterwalder, L. Patthey, J. G. Checkelsky, N. P. Ong, A. V. Fedorov, H. Lin, A. Bansil, D. Grauer, Y. S. Hor, R. J. Cava, and M. Z. Hasan, *Nature (London)* **460**, 1101 (2009).